Tribology Letters (2022) 70: 81
https://doi.org/10.1007/s11249-022-01622-2

ORIGINAL PAPER

Experimental Study on the Expended Energy on Structural Degradation of Lubricating Greases

Leif Ahme[1] · Erik Kuhn[1] · Miguel Ángel Delgado Canto[2]

Received: 3 January 2022 / Accepted: 26 May 2022 / Published online: 17 June 2022

Abstract
One of the keystones of tribological studies is the energetical approach to the lubrication process. In the particular case of lubricating greases, part of the lubrication process's energy dissipates due to a shear-induced structural rearrangement of the 3D network of the thickening agent dispersed in the base oil. This fact confers them a particular consistency, mechanical stability, rheological and tribological behaviour. In this research work, we investigate the mechanical structural degradation induced by shear stress applied in rheological tests (rotational and oscillation mode) and the influence of thickener (type and composition) and base oil on both the degradation process and the expended mechanical energies. For this purpose, lithium, calcium and polyurea-based greases of NLGI grade 2 were used. These greases have been manufactured with a different base oil (mineral, synthetic and vegetable oils) and kinematic viscosity of 48 or 240 mm^2/s. Some biogenic greases were also included in this research. The optical microscopy analysis revealed thickener particles-based agglomerates with different shapes and sizes that reduced notably, if not almost completely destroyed, after stress. Due to the thickener particles-based agglomerates distribution, significant differences in the shear-induced frictional energy inside the bulk grease during the shear process were detected. The size of agglomerates depended on both the thickener content and the base oil viscosity and not the type of base oil.

Keywords Lubricating greases · Shear-induced structural degradation · Energetic approach · Microscopy · Rheology

1 Introduction

Lubricating greases are semi-solid lubricants with a markedly viscoelastic behaviour [1]. We find usability in various applications, especially in ball bearings under boundary or mixed friction.

Lubricating greases have a significant behaviour under friction stress compared with lubricating oils. There are many investigations of the particular tribological and rheological behaviour [2–5]. The Non-Newtonian behaviour, characterised by thixotropy, yield stress and viscoelastic behaviour, are the main differences compared with others [6].

✉ Leif Ahme
leif.ahme@haw-hamburg.de

[1] Department of Mechanical Engineering and Production Management, Hamburg University of Applied Sciences, Hamburg, Germany

[2] Department of Chemical Engineering, University of Huelva, Huelva, Spain

Lubricating greases are classified by the consistency gained by their microstructural skeleton developed by the thickener agent, according to the ASTM D217. This viscoelastic lubricant is generally a highly 3D structured suspension consisting of 70–90 wt% of base oil (mineral, synthetic or vegetable oil) and 3–30 wt% of thickener agent and additives [7]. The thickener is added to increase the consistency of greases and prevent loss of lubricant under operating conditions, but this implies a considerable resistance to the flow of these materials. Furthermore, the thickener forms an interconnected network, characterised by physical bonds like H-bridge or Van der Waals forces and stearic hindrances, which trap the oil and confers the appropriate rheological and tribological behaviour to the grease. As Delgado et al. [1] pointed out, this structural skeleton (size and shape of the disperse phase particles) is hugely affected by the processing conditions and grease composition (mainly, thickener content and base oil viscosity).

Since lubrication is mainly a deformation and flow problem, the knowledge of the rheological properties of lubricating greases may contribute to elucidating one of the

unresolved problems in tribology: the effect of viscoelasticity on the friction process and, consequently, how a lubricating grease behaves under lubricating conditions. Thus, greases undergo structural degradation due to friction stress, which divides into two groups—mechanical degradation and chemical degradation. Some attempts were made to analyse the grease-based friction process through rheological measurements. Thus, Delgado et al. [8] and Kuhn [9] stated that grease elastic deformation, thickener particles' reversible orientation and the final, irreversible dispersion of these particles in the oil could be attributed to progressive changes in the structure of the grease when it is transferred to the friction process. They developed an approach to study the structural degradation of lithium greases in the friction process using stress-growth experiments. This test displayed a decreasing energy expenditure during the shear process until a steady-state situation was reached, i.e. a stationary non-equilibrium state. This intrinsic reaction of the observed mechanical degradation is an expression of a general effort of energetically stressed systems [10, 11]. It means that the stressed lubricating grease is pushed into a non-stable situation and looks for a possibility to get an energetic release. Consequently, a change of the grease structure is involved as a path to minimise the energetic gradients to reach a stable situation.

In this context, Roman et al. [12] showed that grease microstructure was influenced by shear rate and shear time with the help of AFM and SEM micrographs. Paszkowski and Olsztynska-Janus [13] found a process of destroying H-bonds between Li-soap fibres during shear stress by a rheometer. In addition, the quantitative description of the structural degradation caused by mechanical energy can be found in different ways. Bryant, Khonsari and Ling [14] first defined the term “degradation coefficient”. They described it as the generalised thermodynamic and degradation forces ratio. It can elucidate the rates associated with the degradation equation based on the entropy concept and degradation process rather than process variables. Rezasoltani and Khonsari [5] used entropy generation and penetration measurements to define the mechanical degradation of lubricating greases. Osara and Bryant [15] did an extensive investigation from a thermodynamic point of view. They describe the so-called degradation coefficient for lubricating greases by applying the degradation-entropy generation theorem to phenomenological entropy generation for stressed greases. Finally, the work done by Zhou [4] delivers a Master curve. Softening of grease as a function of shear rate, temperature, time and use of the input energy density were investigated.

In this paper, we investigate the mechanical degradation observed in the rheometer tests from the point of view of the changes in the structural skeleton confirmed by the thickener as a consequence of shear stress applied, and we study the influence of thickener (type and composition) and base oil on the degradation process. We only investigate the effect of mechanical energy (shear process); other influences such as thermal energy chemical energy are neglected.

2 Materials and Experimental Methods

2.1 Materials

Ten different lubricating greases differing in composition were tested. The type and concentration of thickener and type and viscosity of the base oil were specifically selected because they influence grease microstructural and rheological behaviour [1]. All of them were NLGI group 2 that soap concentration had to be modified appropriately to get this NLGI grade. Although the soap concentration changes the rheology of greases, the influence is proportional and can be controlled [1].

No additives were included to exclude other possible effects on structural degradation. Greases were classified into two groups. The first group with conventional greases is based on metal soap and polyurea (C1–C4 lithium greases; C5–6 calcium greases, and C7 polyurea grease). The second group are newly developed pure biogenic lubricating greases based on vegetable oil and a combination of lignocellulosic material, esters compound and beeswax as a thickener (B1–B3). The composition of the different lubricating greases analysed in this study and their basic properties are listed in Tables 1 and 2, respectively. Greases were kindly supplied by Fuchs Europe Schmierstoffe (Mannheim, Germany) and Fuchs Lubritech (Kaiserslautern, Germany) as part of the TriBioGen research project. The biogenic lubricating greases were investigated in various studies by Acar [16, 17]. The most promising ones were recommended for further investigation, and therefore, samples B1–B3 were selected for this work.

2.2 Microscopy Measurements

A transmitted light microscope from Olympus (Hamburg, Germany) was used to evaluate both unstressed and stressed structural skeletons of lubricating greases. A very thin layer was spread on a specimen's standard glass-based holder to get transmitted light microscope samples. At least three different fresh samples of each grease were analysed, taking five pictures at various locations to obtain a natural representative morphology for each grease studied. The objective used was a Plan Achromat objective (PLCN20x) from Olympus, specially designed for liquid substances with a 20 × magnification. An Olympus DP27 digital camera with 6.3 × magnification was used to take the images at room temperature, giving a cumulative magnification of 126. At the bottom right of all images, the white scale indicates 100 µm

Table 1 Conventional lubricating greases

Lubricating greases	Thickener type	Thickener concentration [%]	Base oil	Base oil viscosity at 40 °C [mm^2/s]	NLGI grade	Dropping point [°C]
C1	Lithium-12-hydroxystearate	16.1	Castor oil	240	2	≈190,111
C2	Lithium-12-hydroxystearate	10.6	PAO	240	2	≈210,497
C3	Lithium-12-hydroxystearate	13	PAO	48	2	≈208,479
C4	Lithium-12-hydroxystearate	9.5	Mineral oil	240	2	≈206,493
C5	Calcium-12-hydroxystearate	9.7	Castor oil	240	2	≈142,055
C6	Calcium-12-hydroxystearate	22.8	PAO	240	2	≈150,872
C7	Polyurea	19.6	PAO	240	2	≈296,913

Table 2 Biogenic lubricating greases

Lubricating greases	Thickener type	Thickener concentration [%]	Base oil	Base oil concentration [%]	Base oil viscosity at 40 °C [mm^2/s]	NLGI grade	Dropping point [°C]
B1	Cellulose	1.5	Glycerine	88.5	227.4	1	< ≈100?
			Glyceryl-monooleate	10	120.1		
B2	Polyhydroxy butyrate	5.3	MCT oil	55	14.7	0–1	≈80
	Ethylcellulose	7.7	Castor oil	22	258.3		
			HOSO	10	46.2		
B3	Beeswax	7	HOSO	50	46.2	00	≈45
	Glycerol monostearate	5	Castor oil	36	258.3		
	Cetyl alcohol	2					

at the magnification. It is worth mentioning that much effort was made to ensure a similar illumination for all images captured. Despite this, some samples showed slight differences in brightness, which made it impossible to find an illumination time suitable for all areas of these samples. In these cases, the so-called High Dynamic Range (HDR) image recordings were made, which brought the opportunity to control both brightness and darkness on the image processing software [18].

Morphological observations of each representative grease's microstructure were conducted at room temperature with a scanning electron microscope (SEM), model ZEISS EVO LS15 (ZEISS, Germany), at 10 kV. A magnification of 7000 × was used. Previously, all samples were chemically fixed on the holder with 2.5 wt% glutaraldehyde in 0.1 M cacodylate buffer for two hours, followed by three washes in 0.1 M cacodylate solution. Subsequently, all samples were subjected to a second fixation with one wt% osmium tetraoxide solution for 1 h, again followed by three washes with 0.1 M cacodylate solution. Finally, all samples were submitted to critical point drying in acetone before being metallised with Au/Pd. Representative morphology prototypes were assured by using, for each formulation studied, at least three different samples and taking five pictures at various locations.

Although presenting SEM images, the optical microscope images were deliberately preferred in this experimental study on the expended energy on structural degradation. These images were used to discuss a more applied and macroscopic observation of the structural degradation of the bulk grease and to obtain an overview of the agglomerates.

2.3 Rheological Measurements

The most common friction regimen in most machine elements work is mixed friction. The frictional energy of the overall system results from both solid and liquid friction. Rheological investigations provide accurate data on both the internal friction and the structural degradation of the stressed lubricating greases and lead to measuring the mechanical work expended due to the implemented shearing process.

All rheological tests were performed using a grooved plate–plate geometry of 25 mm diameter and 1 mm gap at constant temperatures of 40 °C (MCR 302) and 80 °C (MCR 300) in controlled-stress rheometers (Anton Paar, Austria). Grooved surfaces were selected to prevent wall slip phenomena [19]. To ensure constant temperature conditions, a Peltier temperature control system (Anton Paar—Peltier systems with TruGap™) with an environmental control chamber, as described above, was used.

The experimental procedure with rheometers was organised in three consecutive steps (Fig. 1). During all rheological measurements, both torque and rotational velocity, among other parameters, were recorded every second and used to quantify the involved mechanical energy on the grease.

In the first step, no strain on the sample was imposed during the 900 s to allow the grease to relax or rather to compensate the squeezing process and, second, to allow the grease to reach the commanded temperature. In previous investigations in our laboratory, it was determined that a rest time of 900 s was enough. In the second step, the sample was stressed within the shear rate range from 0 to 1000 s^{-1} for 7200 s to induce structural changes in the lubricating greases under liquid friction-liked conditions. The long period was selected to achieve a stationary state with all lubricating greases studied. Higher shear rates than 1000 s^{-1} were not considered because a notable leakage phenomenon was appreciated. Finally, a third step consisting of a strain-sweep test in oscillation mode at a constant frequency of 1 Hz was performed within the strain range from 0 to 100%. This oscillation test aimed to determine the shear-induced structural degradation rate in the previous rotational test by analysing the strain region below the crossing point of G′ and G″ (frequency at G′ = G″) was reached. We consider that the energy expended to reach the crossing point of G′ and G″ is an indirect indicator of grease structural degradation. The strain-sweep test in oscillation mode was also carried out on unstressed greases for comparative purposes. Three replicates were performed on fresh samples for each grease to ensure the accuracy of the results. The results have shown a statistical significance at a 95% confidence level. In addition, a mean value was calculated for all three outcomes.

3 Results and Discussion

3.1 Basics of Energetic Calculation

The data from rheological tests (rotational and oscillation mode) were used to determine the expended energy under shear stress conditions. This energy is shear-induced frictional energy inside the bulk grease due to a structural rearrangement process quantified as mechanical work. Thus, rotational mode implies flow conditions. The energy supplied into the lubricating greases during the test leads to structural degradation of the grease, apart from a portion of it is dissipated as heat energy. On the other hand, the oscillation mode allows the expended mechanical work to analyse the shear-induced structural changes to achieve a predominant liquid-like behaviour. The thickener (type and composition) and the base oil affect the shear-induced structural changes (i.e. the expended mechanical energies). Details about the calculation of the mechanical work involved in both rotational (structural degradation) and oscillation (non-degraded structure) tests follow below.

3.1.1 Mechanical Work During the Viscous Flow Transient Test

All greases were stressed using a controlled-stress rheometer, which imposed specific shear stress conditions. Thus, the viscous flow transient test under simple shear conditions may provide a feasible measure of the shear-induced frictional energy on the grease at fixed shear stress.

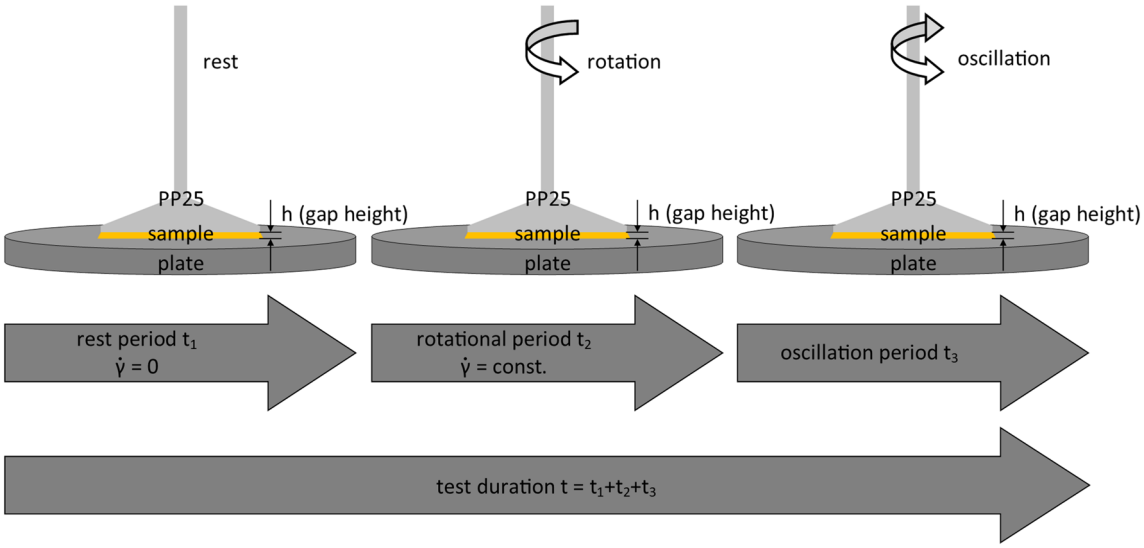

Fig. 1 Schematic illustration of the experimental procedure

The approach of Zhou [4] was used to determine the mechanical work W_R supplied to the sample during the rotational test at a constant shear rate (Eq. 1).

$$W_R = \int_{t_i}^{t_{i+1}} \frac{M_{di} \bullet n_i \bullet 2\pi}{60} dt. \tag{1}$$

The rheological test was programmed to measure a torque value each 15 s within the full-time range studied (7200 s). Therefore, equation one was solved considering a constant segment of time (15 s). Thus, if each segment of time is considered individually with its torque value measured, the total mechanical work during the viscous flow transient test for 7200 s can be calculated as the sum of all segments of time, as follows:

$$W_R = \int_{t_i}^{t_{i+1}} \frac{M_d \bullet n \bullet 2\pi}{60} dt = \sum_{i=1}^{m} \frac{M_{di} \bullet n_i \bullet \pi \bullet \Delta t_i}{30}, \tag{2}$$

with

M_{di} = Measured Torque [Nm].

n_i = Rotational velocity [min^{-1}].

Δt_i = Segment of time [s] (corresponding to each measured point).

m = total number of segments of time within the full-time range studied.

3.1.2 Mechanical Work During Oscillation Test

The oscillation test is widely used to determine the viscoelastic behaviour of the lubricating greases, which is directly related to their structural features [1]. In this test, attention was paid to the intersection of G′ and G″, a transition point from solid-like to liquid-like, i.e. a point above which the grease loses the solid-like behaviour and the liquid-like behaviour becomes dominant. Thus, it will provide information about the structural degradation caused by previously applied shear conditions and how it affected viscoelastic behaviour.

The calculation of the mechanical work in the oscillation test is much more complicated than in the rotational test because, on the one hand, no shear rate was applied. On the other hand, the test runs in oscillating sinusoidal movements. It means that the output values for the shear rate $\dot{\gamma}$ and the torque M_d are always maximum values. Nevertheless, a method was proposed to determine the mechanical work during the test. The effective shear rate is estimated from Eq. 3:

$$\dot{\gamma} = C_{SR} \bullet n, \tag{3}$$

with

$\dot{\gamma}$ = Shear rate [s^{-1}].

C_{SR} = Conversion factor shear rate [s^{-1}/min^{-1}].

n = Rotational velocity [s^{-1}].

The conversion factor of C_{SR} for the respective grooved plate–plate geometry used was determined according to the necessary standard procedure according to Anton Paar with calibration fluid. Thus, the rotational velocity n is estimated from Eq. 4.

$$n = \frac{\dot{\gamma}}{C_{SR}} \tag{4}$$

As values of the shear rate $\dot{\gamma}$ and the torque M_d registered were the maximum values (peak values) reached under the sinusoidal movement, we used an approach from Electrical Engineering. Thus, a rectified value is determined for a sinusoidal current. This corrected value is the occurring mean value of the integral over the amounts of the sine wave [20]. Figure 2 intended to illustrate the situation in more detail.

The sinus curve shows the second oscillation (dotted) reflected upwards. In the figure, $\hat{i}$ represents the peak value and $|\bar{i}|$ represents the rectified value. The following formula gave the ratio of rectification value to peak value:

$$\frac{|\bar{i}|}{\hat{i}} = \frac{1}{T}\int_0^T |\sin(\omega t)| d(\omega t) = \frac{2}{\pi} \sim 0.6366. \tag{5}$$

In our case, the values obtained from the rheometer are peak values, i.e. the shear rate $\hat{\dot{\gamma}}$ and the torque $\widehat{M_d}$. However, rectified values are required to calculate the mechanical work during the oscillation test. These were calculated from Eqs. 6 and 7, respectively:

$$|\bar{\dot{\gamma}}| = \hat{\dot{\gamma}} \bullet \frac{2}{\pi}, \tag{6}$$

$$|\bar{M}_d| = \widehat{M_d} \bullet \frac{2}{\pi}. \tag{7}$$

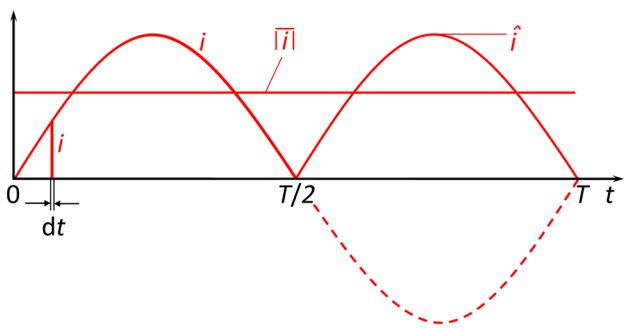

Fig. 2 Sine current curve for a rectified value cf. [20]

Thus, with the help of these adaptations described above, it can successfully determine the mechanical work during the oscillation test by using Eq. 2. Please note that the segment of time, in this case, is not always constant 15 s as in the case of the viscous flow transient test; it varies.

3.2 Structure of Unstressed and Stressed Lubricating Greases

As it is well known, lubricating greases are essentially highly structured two-phase colloidal suspensions consisting of a thickening agent dispersed in a base oil. The thickener forms a three-dimensional gelling network that traps the oil by capillary phenomena and molecular attraction and confers them to the appropriate consistency, rheological and tribological behaviour. Figure 3 shows the SEM micrographs corresponding to representative lithium soap, calcium soap and polyurea-based greases manufactured with the same synthetic oil (PAO 240 mm^2/s). No SEM micrographs of pure biogenic greases studied (B1, B2 and B3) were obtained because their dropping points were much lower. That is why it is technically impossible to observe these samples by SEM. However, all of them showed a high density of entangled soap fibres. Li-soap-based greases showed a spongy and entangled structural skeleton with the largest fibres, while polyurea-based grease showed more heterogeneous soap particles, which looked like aggregates of fibres [1, 6].

However, from a macroscopical point of view, these microstructural skeletons can be organised as agglomerates of different shapes and sizes, demonstrated by optical microscopy, as a consequence of the process of crystallisation of the thickener particles [1]. Figures 4, 5, 6 and 7 show the optical microscopic images of both unstressed and stressed states for lithium, calcium, polyurethane and pure biogenic greases. These visual images differ in colour due to firstly the greases having different primary colours and, secondly, each prepared sample experiences different refraction of the light under the microscope. As can be well appreciated, the structural pattern of unstressed grease was changed into a pattern with a smaller grouping of particles and more oriented toward the flow direction. In addition, as Paszkowski and Olsztynska-Janus [13] and Delgado et al. [6] pointed out, lubricating greases show a highly shear-thinning behaviour for which the structural skeleton undergoes elastic and plastic deformation and even disintegration when a high shear rate is applied. For this aim, optical microscopy images were taken for all greases studied and compared with the knowledge gained from rheological tests to identify further possible correlations between the different components of the model greases, the structural degradation process and the expended mechanical energies involved.

All greases were highly stressed by a transient flow test at 1000 s^{-1} for 22 h using a cone plate of 50 mm diameter to ensure a consistent shear of the sample and avoid any leakage phenomenon characteristic of lubricating greases [6]. After this time, a stressed grease specimen was deposited on a standard glass holder to observe it microscopically. Thus, any possible disturbance of the aggregates pattern was avoided due to the thixotropy effects. As expected, the number of agglomerates decreased and became smaller than unstressed samples, and the aggregate pattern of stressed greases studied was more homogeneous and cohesive (Figs. 4, 5, 6, 7).

Concerning lithium greases (Fig. 4), the characteristic fibre-based microstructural skeleton of lithium greases could not be identified macroscopically with an optical microscope. However, it is noteworthy that numerous lithium soap-based agglomerates with different shapes and sizes can be recognised in the unstressed sample. It was detected that the size of these agglomerates depended on both the soap content and the base oil. Thus, the Li grease with the highest soap content (grease C1) or the lowest oil viscosity (grease C3) showed the most oversized agglomerates. According to Delgado et al. [1], either low-viscosity base oil or high soap content leads to a high density of entanglements with

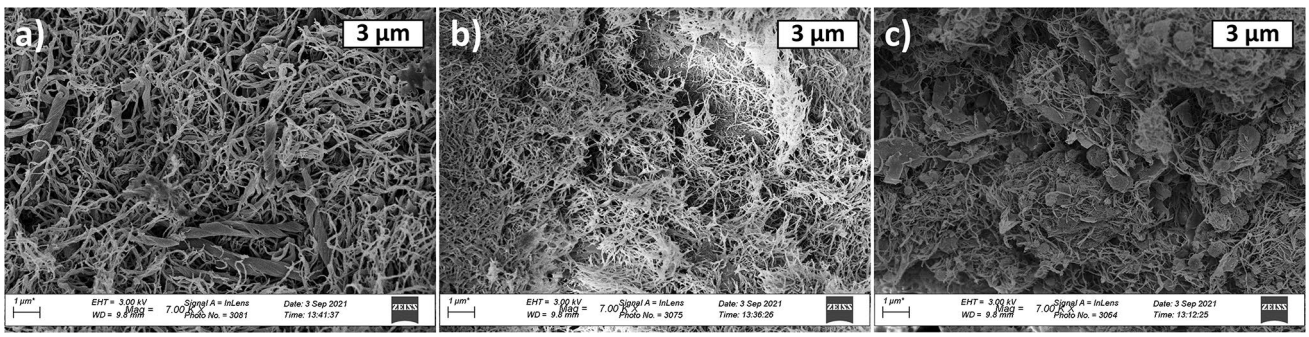

Fig. 3 SEM (15 kV and 7000 magnification) micrographs corresponding to **a** lithium grease (C2); **b** Calcium grease (C6); **c** Polyurea grease (C7)

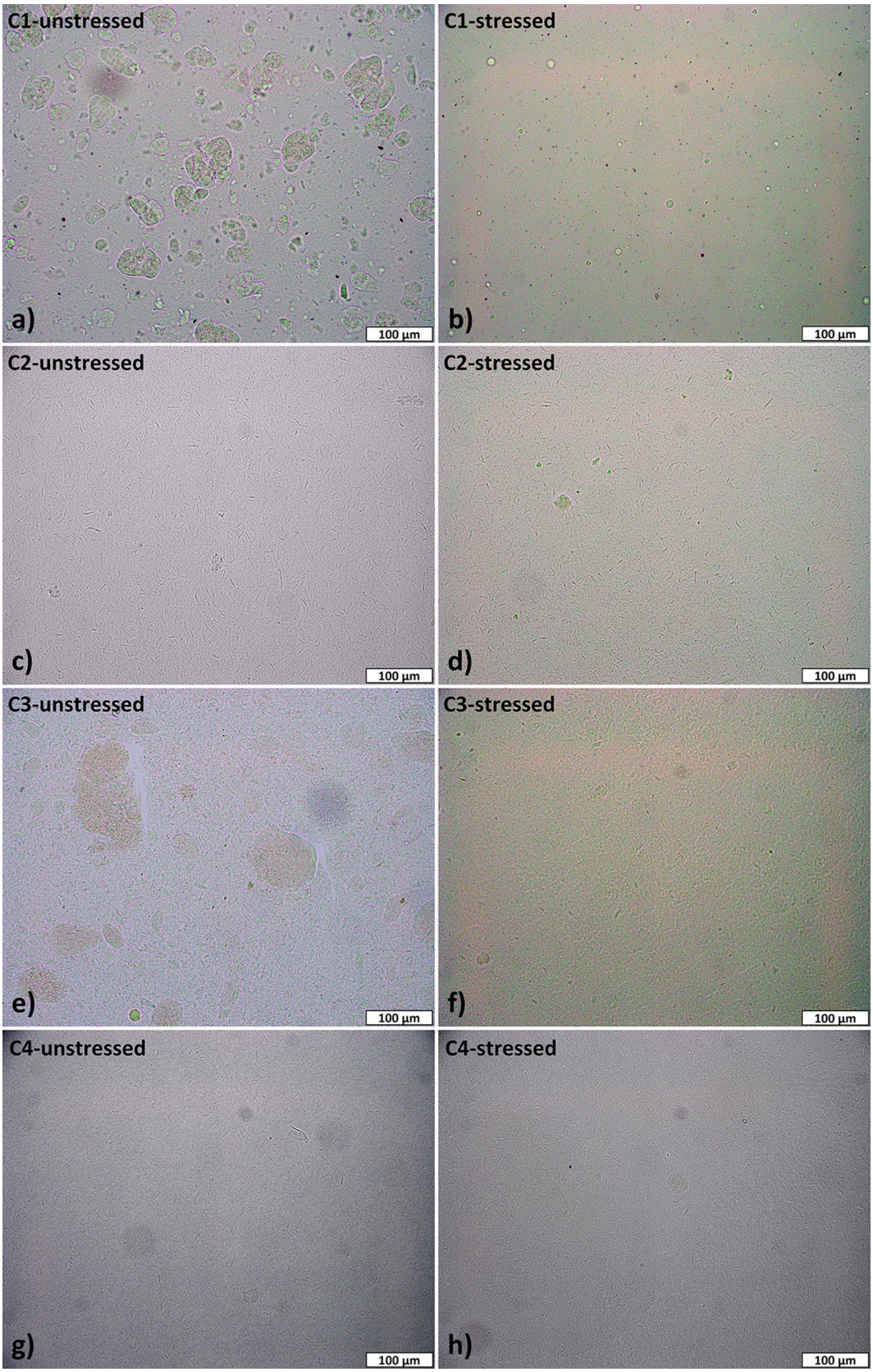

Fig. 4 Optical microscopic images of the lithium greases: **a**, **b** C1; **c**, **d** C2; **e**, **f** C3; **g**, **h** C4—left-side column are unstressed greases and right-side column are stressed greases (1000 s^{-1} for 22 h)

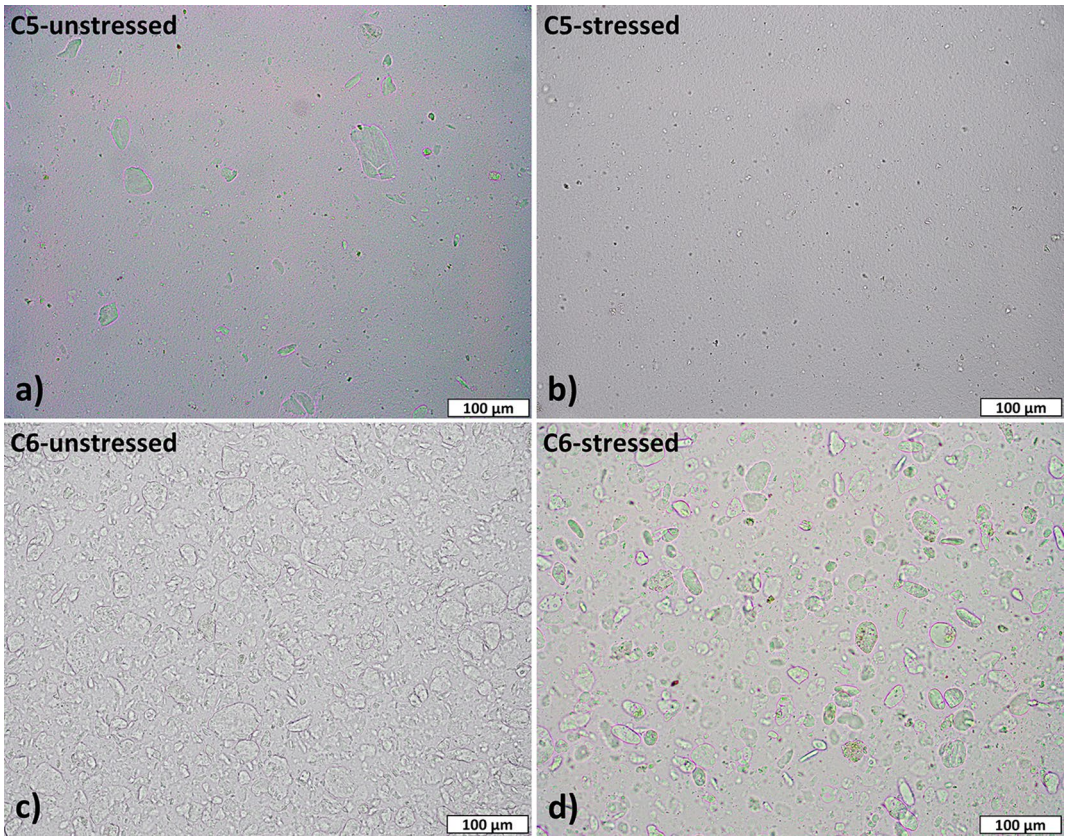

Fig. 5 Optical microscopic images of the calcium greases: **a**, **b** C5; **c**, **d** C6—left-side column are unstressed greases and right-side column are stressed greases (1000 s^{-1} for 22 h)

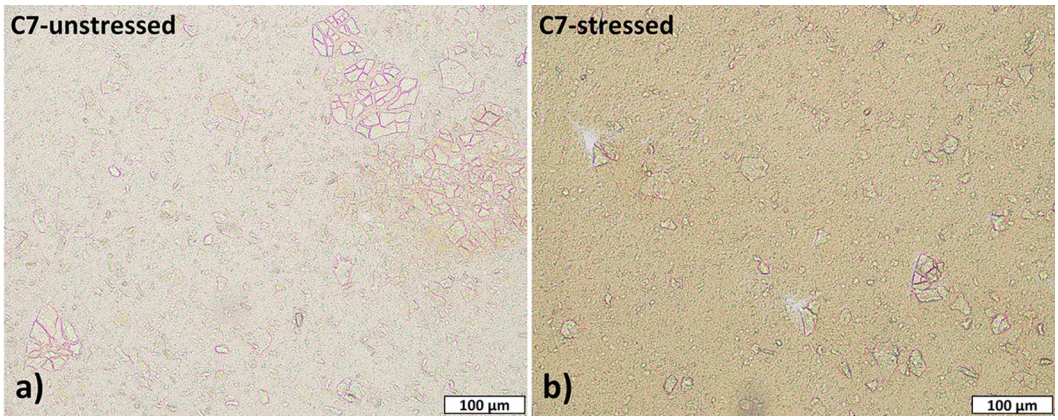

Fig. 6 Optical microscopic images of the polyurea grease (C7) **a** unstressed grease, **b** stressed grease (1000 s^{-1} for 22 h)

a higher shear-structural dependence (low values on flow index). After these lithium greases were highly stressed, lithium soap-based agglomerates were notably reduced, if not almost wholly destroyed.

Concerning calcium greases (Fig. 5), a similar behaviour to lithium greases was observed. Unstressed calcium greases showed uneven thickener agglomerates of different shapes and sizes. Calcium grease with the highest soap content (grease C6) showed a high density of more extensive calcium soap-based agglomerates. Just after stressing, calcium agglomerates' size was highly reduced. Then a comparison between optical images of both unstressed lithium (C1, C2) and calcium (C5, C6) greases was conducted. Both had different soap content and type of base oil (castor oil and PAO)

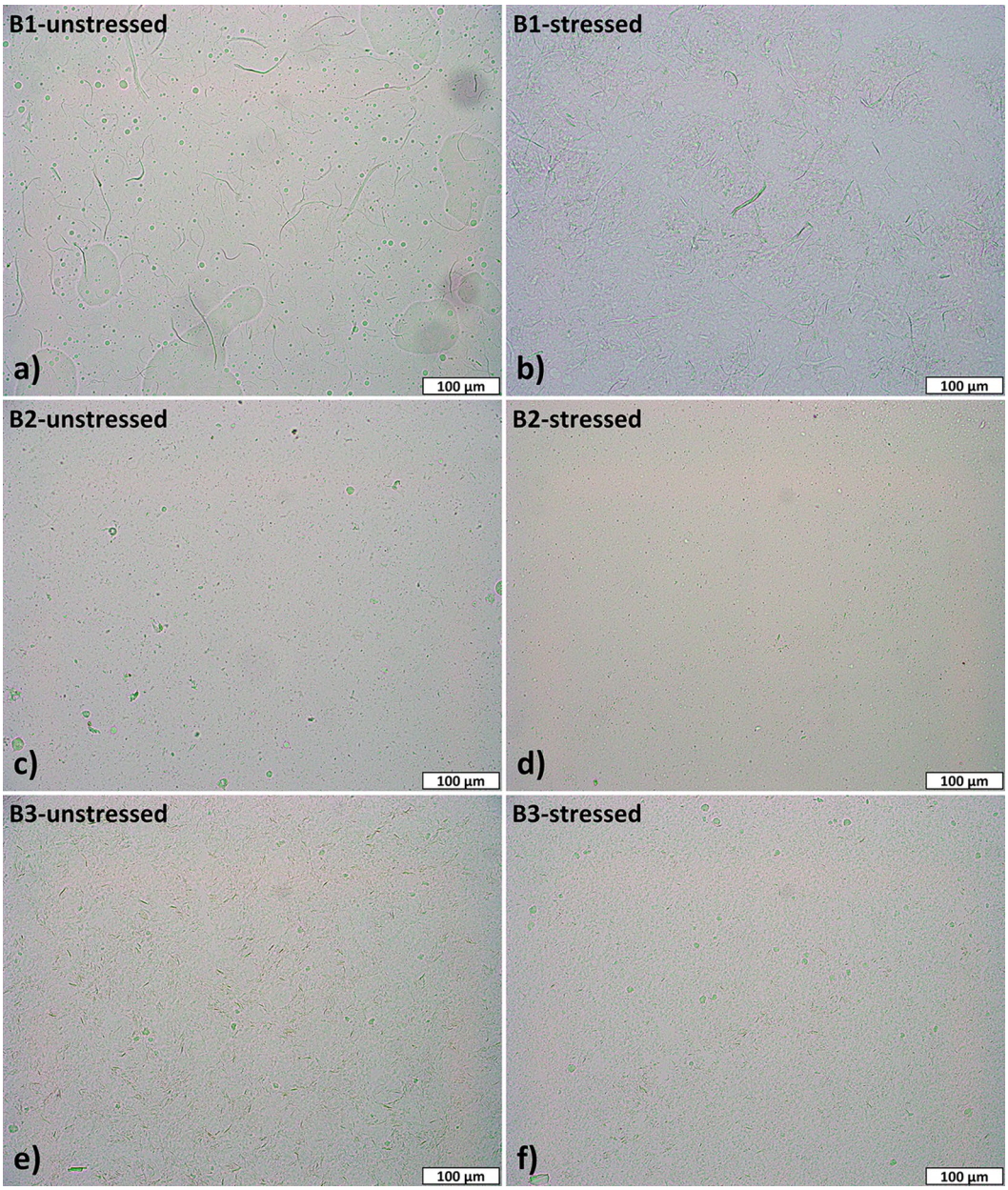

Fig. 7 Optical microscopic images of the pure biogenic greases: **a**, **b** B1; **c**, **d** B2; **e**, **f** B3—left-side column are unstressed greases and right-side column are stressed greases (1000 s^{-1} for 22 h)

with a kinematic viscosity of 240 mm^2/s. It shows that the size of metal soap-based agglomerates was mainly affected by the soap content and not the base oil type. Lithium or calcium greases with the lowest soap content were significantly more homogeneous in an idle state and showed fewer structural changes in the shear stress process.

The polyurea grease (Fig. 6) shows well-defined flakes of different sizes but are not more prominent than those observed for lithium or calcium greases. Unlike both stressed lithium and calcium greases, large agglomerates were kept for stressed polyurea grease, although with reduced and more homogeneous sizes than the unstressed polyurea grease.

Finally, the unstressed pure biogenic greases B1 to B3 studied (Fig. 7) did not present well-defined thickener agglomerates due to the thickener agent used. The cellulose fibres of grease B1 can be easily macroscopically recognised in the unstressed and stressed state. Contrarily to previous non-biogenic greases, the scattered cellulose fibres in the unstressed grease appeared closer after stress. Tiny spots were appreciated in biogenic greases B2 and B3, and their macroscopical structures appear much more homogeneous

after stressing. The particle arrangement looks very homogeneous after the stress, and only a few smaller and shapeless agglomerates are still present.

3.3 Expended Energy to Achieve the Liquid-Like Behaviour

Figures 8 and 9 show the required mechanical work during the oscillation test to achieve a liquid-like behaviour once the grease was stressed at a specific shear rate. Discontinuous lines show the tendency of the measured values, which a logarithm model may conveniently represent except for grease C2 in Fig. 9a. It displays as a function of the shear rate applied at which the greases studied were degraded on the previous rotational test performed. Although the initially examined shear rate range was from 0.1 to 1000 s^{-1}, a non-completely grease degraded structure was reached with lower shear rates than 100 s^{-1} at the test conditions, i.e. it was not reached a steady-state behaviour in all cases. Moreover, biogenic greases B1 and B2 did not provide valuable results at high shear rates due to significant fracture and expulsion phenomena up to 10 s^{-1}. Therefore, only data

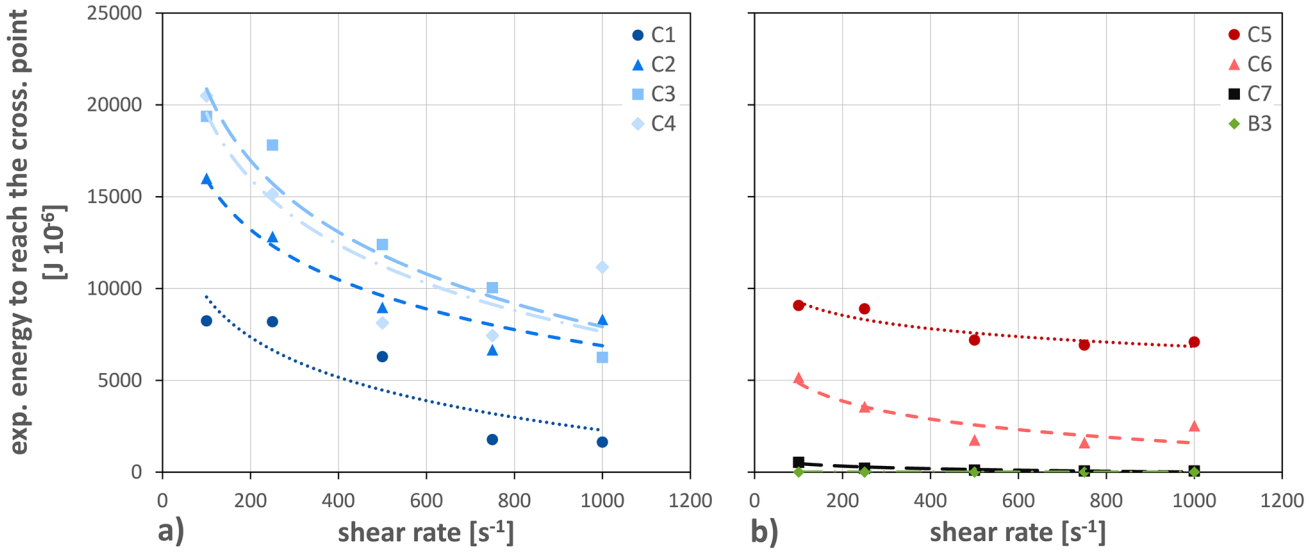

Fig. 8 Expended energy to reach the crossing point at 40 °C for **a** lithium greases and **b** other greases. Logarithm curve fittings are shown by a discontinuous line

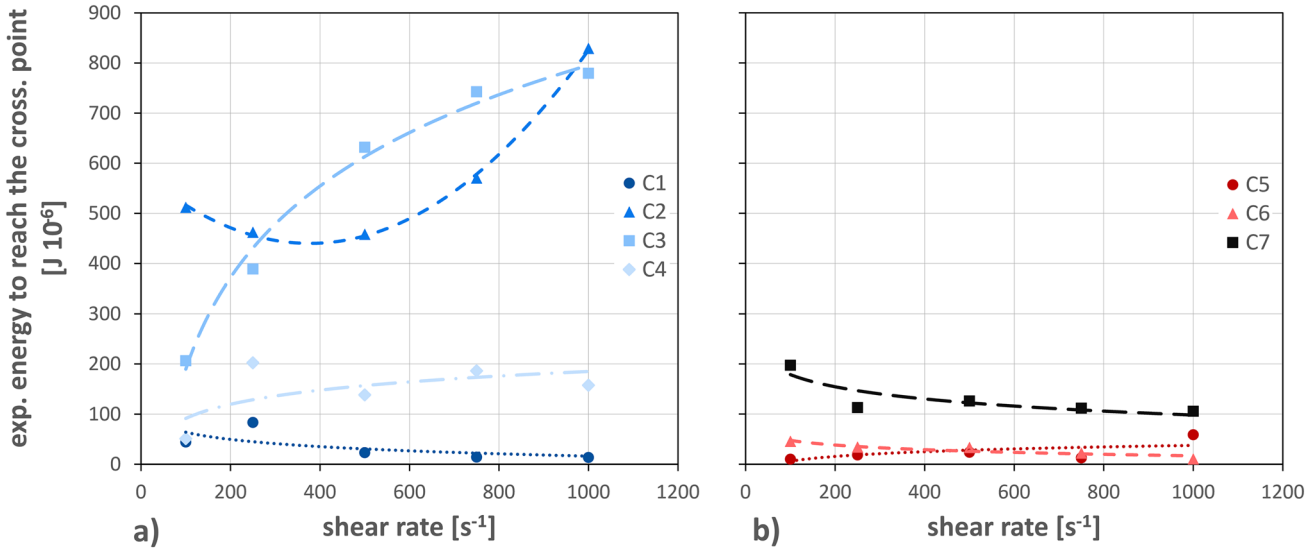

Fig. 9 Expended energy to reach the crossing point at 80 °C for **a** lithium greases and **b** other greases. Logarithm curve fittings (C1, C3, C4, C5, C6, C7) and polynomial curve fitting (C2) are shown by a discontinuous line

obtained from reproducible tests at higher shear rates than 100 s^{-1} were considered in the current study; the steady-state conditions were reached in all plotted cases after 22 h. According to Delgado et al. [6], it is worth mentioning that the shear-induced grease behaviour at these high shear rate ranges should be consistent with the physical degradation produced by the over rolling on the bulk grease close to the contact area.

Y-positions of these curves display the amount of expended energy to reach a specific structural degradation until the crossing point, i.e. the internal frictional energy involved within the grease degradation process starts and keeps the flow process. Thus, the higher the expended energy to reach the crossing point, the higher the internal frictional energy is. The structural features of the greases affect the internal frictional energy (Fig. 3). Consequently, lithium and calcium greases with a spongy and entangled fibres-based structural skeleton showed higher internal friction energies than polyurea grease, which showed matted fibres with barely free-motion space among themselves. On the other hand, the expended energy-shear rate dependence is an indirect expression of the internal structural degradation rate, i.e. the grease wear. It is closely related to the agglomerates' pattern originating from the shear conditions and observed by optical microscopy (Figs. 4, 5, 6, 7).

At 40 °C (Fig. 8), the higher the applied shear rate was, the lower the expended energy reached the crossing point between G′ and G″, regardless of the evaluated greases. It suggested a lower internal frictional energy to achieve the liquid-like behaviour as much stressed the lubricating grease was, i.e. as much degraded the structural pattern of the grease was. It is noteworthy that lithium, calcium and polyurea showed significant differences in the expended energy to reach the crossing point, despite being NLGI grade 2. In general, the degradation of the bulk structural skeleton of lithium greases showed a strong dependence on the shear rate applied. However, biogenic, polyurea and calcium greases, which showed fewer differences in the structural patterns between unstressed and stressed greases, hardly displayed any variation of the expended energy within the shear rate range studied. Therefore, the type of structural pattern highly affects the internal frictional energy involved in the grease degradation process to start and keep the flow process even more than the thickener content and the oil viscosity. Thus, Li-soap-based greases developed a high internal frictional energy within the structural rearrangement process to start to flow because their internal network is based on larger fibres forming a well-entangled structural skeleton (Fig. 3) [6]. Moreover, they also showed a higher internal wear rate than other greases studied.

On the other hand, greases with the highest thickener contents tested: C1 (16.1 wt%), C6 (22.8 wt%) and C7 (19.6 wt%), required less energy to flow than their grease counterpart with lower thickener content. Thus, lithium greases C3 (13 wt%) and C4 (9.5 wt%) showed the highest expended energies to reach the crossing point. In addition, Li grease C3, produced with the lowest oil viscosity (48 mm^2/s), implied the highest expended energy to start to flow and the highest internal structural degradation rate within the shear rate studied. As previously pointed out by Delgado et al. [1], the oil viscosity induced differences in the structural skeleton network of lithium grease, such as the lower oil viscosity is, the larger affected the structural skeleton by the shear rate. Contrarily, biogenic (B3) and polyurea (C7) greases developed a more intensive structural degradation, affecting their internal grease wear within the studied shear rate range. In addition, it is worth mentioning that the use of castor oil (greases C1 and C5) attenuates the expended energy-shear rate dependence of its grease group because of the molecular attraction between the hydroxyl groups present in both the 12-hydroxystearate of the thickener and the ricinoleic fatty acid in castor oil. Therefore, a suitable interaction between thickener and base oil is helpful to preserve the internal structural degradation within the shear rate applied.

At 80 °C (Fig. 9), the amount of expended energy to reach a specific structural degradation until the crossing point drastically decreased compared to 40 °C. It could be a consequence of, on the one hand, a decrease in the internal binding forces due to the external input of thermal energy; on the other hand, the viscosity reduction caused by temperature increase facilitated the bleeding oil. Only the lubricating grease C7, which showed the highest dropping point, was relatively unaffected within this temperature range. Moreover, the expended energy-shear rate dependence showed a completely different behaviour for lithium greases C2–C4 than at 40 °C. They all displayed increased expended energy to reach the crossing point with the shear rate applied, which evidence a different structural degradation process for lithium greases manufactured with mineral or synthetic oil. It appears as if the introduction of thermal energy stimulated a structural rebuilding process. We think that a total change in the grease structure occurred with temperature due to the separation of the components (thickener and base oil); it is highly affected by the base oil selected. This phenomenon was distinct in the lithium grease manufactured with PAO with the lowest oil viscosity (C3). Only the lithium greases manufactured with castor oil (C1) and the calcium and polyurea greases (C5–C7) displayed an almost similar behaviour with the applied shear rate, although less pronounced than at 40 °C.

Nevertheless, these remarkable results at 80 °C should be considered cautiously because this notable reduction in the internal frictional energy with temperature may facilitate leakage from the gap at high shear rates. Moreover, the grease wear process emphasised that it is almost constant

over the shear rate for nearly all the greases shown (less slope of the curves than 40 °C). Therefore, it is worth pointing out that temperature drastically affected the expended energy-shear rate dependence of Li grease, mainly when PAO was used, and not to the calcium and polyurea greases.

Unfortunately, the biogenic grease reacted more sensitively to rising temperature and became too soft when mechanically stressed at 80 °C, even though it appeared pretty solid at rest (at room temperature). Since measurements at 80 °C hardly provided any relevant results, they are not shown below.

3.4 Ratio of Expended Energies

Follow with the analysis of the energetical approach to structural degradation of lubricating greases; it is interesting to relate the mechanical energy involved within the grease degradation process to start and keep the flow process (W_{CP}), with the mechanical energy involved in the structural degradation achieved along with the viscous flow transient test at a specific shear rate (W_R). Thus, R_{tee} allows a holistic interpretation of the expended mechanical energy involved in the structural degradation that occurred in the stressed grease (Eq. 8).

$$R_{tee} = \frac{W_{CP}}{W_R}, \tag{8}$$

with

R_{tee} = Ratio of the total expended energy.

W_{CP} = Mechanical work until the crossing point at the oscillation test [J].

W_R = Mechanical work supplied from the viscous flow transient test [J].

As commented above, the higher the shear rate is, much mechanical energy was put into the grease to destroy the structure skeleton during the viscous flow transient test. Consequently, it was easier to reach the crossing point at the oscillation test. Thus, the larger the ratio of expended energies is, the less structural degradation occurred in the stressed grease. It means either more energy was required to reach the crossing point or less mechanical energy dissipated during the rotation test.

Figures 10 and 11 show the expended energies ratio versus the shear rate applied at 40 °C and 80 °C, respectively. In these figures, discontinuous lines show the tendency of the measured values, which power curves may conveniently represent. In these cases, the full shear rate range studied was from 0.1 to 1000 s^{-1} and considered to display the full shear rate range studied. As identified, the expended energies ratio drastically decreased within the shear rate range lower than 100 s^{-1}, regardless of the temperature level. After 100 s^{-1}, an asymptotic tendency appeared. This fact suggested that the maximum shear-induced structural degradation of greases reached around 100 s^{-1}. According to Delgado et al. [6], it is an asymptotic tendency of stress-growth behaviour for lithium greases.

At 40 °C (Fig. 10), lithium and calcium greases showed higher values of R_{tee} along the shear rate range studied than polyurea grease (C7) and biogenic greases (B3). The structural skeleton of lithium and calcium greases dissipated less mechanical energy during the rotation test than polyurea and biogenic greases. On the other hand, it reveals that lubricating greases with a higher thickener content led to lower values of R_{tee}, which means more structural

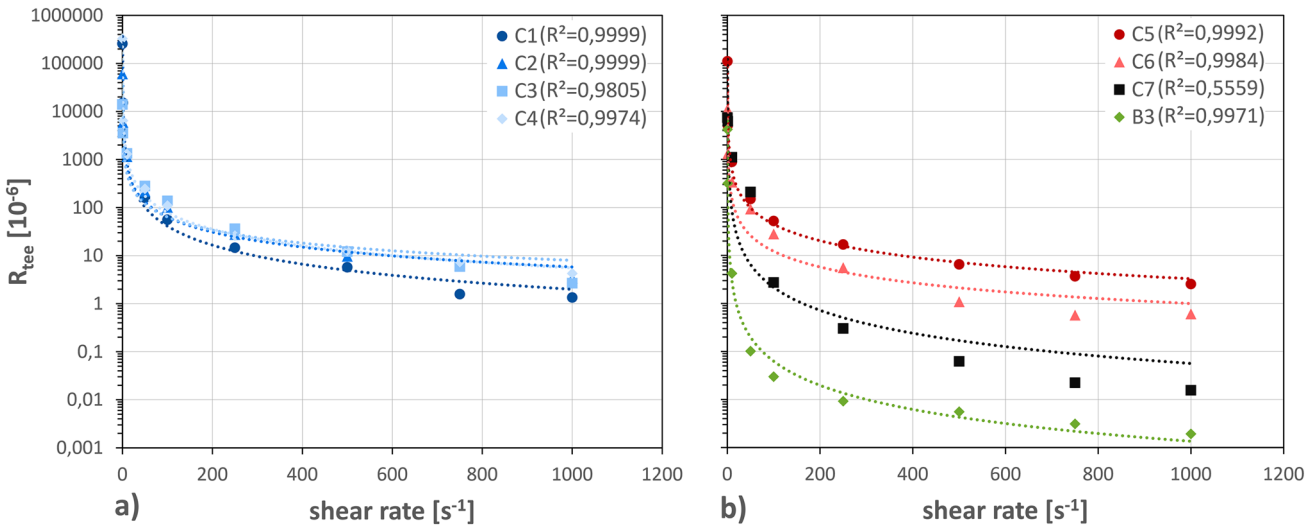

Fig. 10 Ratio of expended energies (R_{tee}) 40 °C for **a** lithium greases and **b** other greases. Power curve fittings are shown by a discontinuous line indicating each R-squared (R^2) in the legend

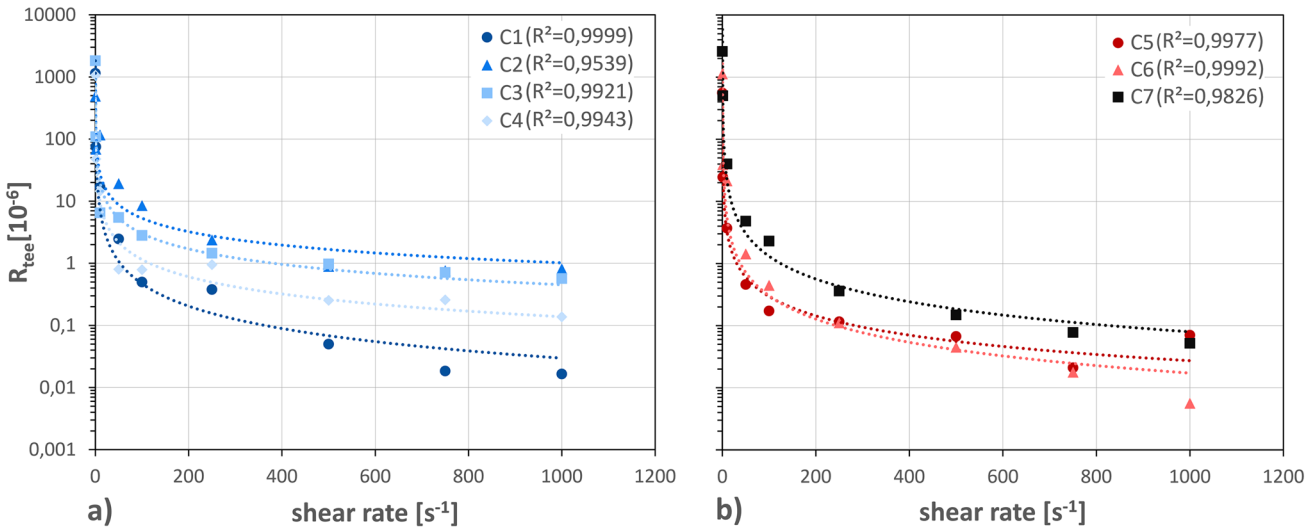

Fig. 11 Ratio of expended energies (R_{tee}) at 80 °C for **a** lithium greases and **b** other greases. Power curve fittings are shown by a discontinuous line indicating each R-squared (R^2) in the legend

degradation in the stressed grease. As commented above, R_{tee} allows a better interpretation of the expended mechanical energy involved in the structural degradation that occurred in the stressed grease. Thus, polyurea grease (C7) and the biogenic greases (B3), which exhibited similar variations of the expended energy to reach the liquid-like behaviour, are far apart in terms of their expended energy ratio. Such as, less structural degradation occurred in the stressed polyurea grease than in the stressed biogenic greases (B3). Therefore, biogenic greases (B3) expended the most mechanical energy to degrade their structural skeleton during the viscous flow transient test compared to the mechanical energy consumed to reach the liquid-like behaviour.

At 80 °C (Fig. 11), the expended energy ratio was substantially smaller than at 40 °C. It was linked with a significant reduction of the internal frictional energy to reach the liquid-like behaviour compared to the mechanical energy supplied into the lubricating greases during the viscous flow transient test. It is worth mentioning that lithium and calcium greases showed more significant differences in the expended energy ratio at 80 °C, with a drastic reduction for the calcium greases. However, the expended energy ratio of polyurea grease (C7) was hardly affected by temperature. It suggests that polyurea grease's structural skeleton better supports the shear-induced structural degradation within this temperature range studied than the other greases. Therefore, this energetical approach could be a suitable measurement of the mechanical stability of the lubricating greases according to the shear-induced structural changes.

4 Conclusion

This work highlights a better understanding of the influence of grease composition (thickener and base oil) on the macroscopically structural degradation of lubricating greases. In addition, it proposes a holistic interpretation of the expended energy involved in the internal structural degradation that occurred in the stressed grease. This expended energy, quantified as a mechanical work from the rheological test, measures the grease wear process, i.e. the shear-induced frictional energy inside the bulk grease.

Despite all traditional model greases studied being NLGI grade 2, they showed significant differences in the structural pattern of unstressed grease obtained by optical microscopy and the expended energy of the stressed greases to start the flow process. Numerous thickener-based agglomerates with different shapes and sizes were recognised in the unstressed sample. Furthermore, the size of these agglomerates depended on thickener content and base oil. Moreover, the type of thickener, which affects the microstructural skeleton, highly affects this internal frictional energy, even more than either thickener content or the base oil. It is worth pointing out that R_{tee} could be a suitable measurement of the expended mechanical energy by structural degradation of the lubricating greases according to the observed shear-induced structural changes. Thus, the larger the ratio of expended energies is, the less structural degradation occurred in the stressed grease. It means that either more internal friction energy is expended to start to flow (reach the crossing point) or

less mechanical energy is dissipated during the structural degradation of the stressed grease. Therefore, this work reveals that the structural skeleton of lithium and calcium greases dissipated less mechanical energy during the shearing process than polyurea and biogenic greases (B3). The stressed biogenic greases (B3) dissipated the highest amount of mechanical energy. In addition, it is noteworthy that lubricating greases with higher thickener content led to lower values of R_{tee}, which means more structural degradation in the stressed grease. On the other hand, the R_{tee} of polyurea grease was hardly affected by temperature, suggesting that the structural skeleton of polyurea grease better supports the shear-induced structural degradation within the temperature range studied than the other lubricating greases.

Author Contributions All authors contributed to the study conception and design. Material preparation, data collection and analysis were performed by Leif Ahme. The first draft of the manuscript was written by Leif Ahme, and all authors commented on previous versions of the manuscript. All authors read and approved the final manuscript.

Funding Open Access funding enabled and organized by Projekt DEAL. The authors did not receive support from any organisation for the submitted work. No funding was received to assist with the preparation of this manuscript. No funding was received for conducting this study. The authors declare that no funds, grants or other support were received during the preparation of this manuscript.

Declarations

Conflict of interest The authors have no relevant financial or non-financial interests to disclose. The authors have no competing interests to declare that are relevant to the content of this article. All authors certify that they have no affiliations with or involvement in any organisation or entity with any financial interest or non-financial interest in the subject matter or materials discussed in this manuscript. The authors have no financial or proprietary interests in any material discussed in this article.

References

1. Delgado, M.A., Valencia, C., Sánchez, M.C., Franco, J.M., Gallegos, C.: Influence of soap concentration and oil viscosity on the rheology and microstructure of lubricating greases. Ind. Eng. Chem. Res. (2006). https://doi.org/10.1021/ie050826f
2. Paszkowski, M.: Assessment of the effect of temperature, shear rate and thickener content on the thixotropy of lithium lubricating greases. Proceed. Instit. Mechan. Eng. Part J J. Eng. Tribol. (2013). https://doi.org/10.1177/1350650112460950
3. Sánchez, R., Valencia, C., Franco, J.M.: Rheological and tribological characterization of a new acylated chitosan-based biodegradable lubricating grease: a comparative study with traditional lithium and calcium greases. Tribol. Trans. (2014). https://doi.org/10.1080/10402004.2014.880541
4. Zhou, Y.: On the mechanical ageing of lubricating greases, University of Twente (2018)
5. Rezasoltani, A., Khonsari, M.M.: On the correlation between mechanical degradation of lubricating grease and entropy. Tribol. Lett. (2014). https://doi.org/10.1007/s11249-014-0399-8
6. Delgado, M.A., Secouard, S., Valencia, C., Franco, J.M.: On the steady-state flow and yielding behaviour of lubricating greases. Fluids (2019). https://doi.org/10.3390/fluids4010006
7. Delgado, M.A., Sánchez, M.C., Valencia, C., Franco, J.M., Gallegos, C.: Relationship among microstructure, rheology and processing of a lithium lubricating grease. Chem. Eng. Res. Des. (2005). https://doi.org/10.1205/cherd.04311
8. Delgado, M.A., Franco, J.M., Kuhn, E.: Effect of rheological behaviour of lithium greases on the friction process. Indus. Lubricat. Tribol. **60**, 37–45 (2008)
9. Kuhn, E.: Correlation between system entropy and structural changes in lubricating grease. Lubricants (2015). https://doi.org/10.3390/lubricants3020332
10. Kuhn, E.: Application of a thermodynamic concept for the analysis of structural degradation of soap thickened lubricating greases. Lubricants (2018). https://doi.org/10.3390/lubricants6010007
11. Abdel-Aal, H.A.: Thermodynamic Modeling of Wear. In: Wang, Q.J., Chung, Y.-W. (eds.) Encyclopedia of Tribology, pp. 3622–3636. Springer, US, Boston, MA (2013)
12. Roman, C., Valencia, C., Franco, J.M.: AFM and SEM assessment of lubricating grease microstructures: influence of sample preparation protocol, frictional working conditions and composition. Tribol. Lett. (2016). https://doi.org/10.1007/s11249-016-0710-y
13. Paszkowski, M., Olsztyńska-Janus, S.: Grease thixotropy: evaluation of grease microstructure change due to shear and relaxation. Indus. Lubricat. Tribol. (2014). https://doi.org/10.1108/ILT-02-2012-0014
14. Bryant, M., Khonsari, M., Ling, F.: On the thermodynamics of degradation. Proceedings of The Royal Society A: Mathematical, Physical and Engineering Sciences (2008). https://doi.org/10.1098/rspa.2007.0371
15. Osara, J.A., Bryant, M.D.: Thermodynamics of grease degradation. Tribol. Int. (2019). https://doi.org/10.1016/j.triboint.2019.05.020
16. Acar, N., Kuhn, E., Franco, J.M.: Tribological and rheological characterization of new completely biogenic lubricating greases: a comparative experimental investigation. Lubricants (2018). https://doi.org/10.3390/lubricants6020045
17. Acar, N., Franco, J.M., Kuhn, E., Gonçalves, D.E.P., Seabra, J.H.O.: Tribological investigation on the friction and wear behaviors of biogenic lubricating greases in steel-steel contact. Appl. Sci. (2020). https://doi.org/10.3390/app10041477
18. Olympus Europa SE & CO. KG: OLYMPUS Stream Online-Help. Stream 2.2. OLYMPUS EUROPA SE & CO. KG, Hamburg (2016). Accessed 14 Oct. 2020
19. Kuhn, E.: Zur Tribologie der Schmierfette. Eine energetische Betrachtungsweise des Reibungs- und Verschleißprozesses, 2nd edn. expert Verlag, Renningen (2017)
20. Fricke, H., Frohne, H., Vaske, P.: Grundlagen der Elektrotechnik. Elektrische Netzwerke, 17th edn. Teubner, Stuttgart (1982)